Published in final edited form as:
*Ultrasound Med Biol*. 2014 December ; 40(12): 2819–2829. doi:10.1016/j.ultrasmedbio.2014.07.005.

# Preliminary *in vivo* breast vibro-acoustography results with a quasi 2-dimensional array transducer: a step forward towards clinical applications

**Mohammad Mehrmohammadi**[1], **Robert T. Fazzio**[2], **Dana H. Whaley**[2], **Sandhya Pruthi**[3], **Randall R. Kinnick**[1], **Mostafa Fatemi**[1], and **Azra Alizad**[1,3,*]

[1] Department of Physiology and Biomedical Engineering, Mayo Clinic, College of Medicine, 200 First St. SW, Rochester, Minnesota, USA

[2] Department of Radiology-Diagnostic, Mayo Clinic, College of Medicine, 200 First St. SW, Rochester, Minnesota, USA

[3] Department of Internal Medicine, Mayo Clinic, College of Medicine , 200 First St. SW, Rochester, Minnesota, USA

## Abstract

We have previously investigated the application of a novel imaging modality, vibro-acoustography (VA) using an annular confocal transducer (confocal VA), integrated into a clinical prone stereotactic mammography system to detect various breast abnormalities. To shorten the scanning time and provide improved coverage of the breast, we have evolved our imaging system by implementing VA on a clinical ultrasound scanner equipped with a “quasi-2-dimensional” array transducer. We call this technique “quasi-2D vibro-acoustography” (Q2DVA). A clinical ultrasound scanner (GE Vivid 7) was modified to perform both ultrasound (US) imaging and VA using an array transducer consisting of a matrix of 12 rows by 70 columns of ultrasound elements. The newly designed system was used to perform VA on patients with either benign or cancerous lesions. Our results indicate that benign and malignant solid breast lesions were easily detected using our newly modified VA system. It was also possible to detect micro-calcifications within the breast. Our results suggest that with further development, Q2DVA could provide high-resolution diagnostic information in the clinical setting and may be used either as a stand-alone or as a complementary tool in support of other clinical imaging modalities.



* Corresponding author: 200 First St. SW, Rochester, Minnesota, USA, phone: +1 (507)538-1727, fax: +1 (507)266-0361, alizad.azra@mayo.edu.



Conflict of interest statement

Mayo Clinic and some of the co-authors (MF) have financial interests associated with the technology used in this research; the technology has been licensed in part to industry.

**Keywords**

vibro-acoustography; breast cancer; ultrasound; *in vivo*; quasi-2D array transducer

## Introduction

Reliable identification and differentiation of breast masses is a challenge of the modern breast imaging practice. Due to the high incidence and mortality rates of breast cancer (Siegel, Naishadham 2013), significant effort has been devoted to development and testing new diagnostic tools to detect, localize, and characterize breast lesions (Adler, Carson 1990, Berg, Zhang 2012, Bluemke, Gatsonis 2004, Corsetti, Houssami 2011, Gordon and Goldenberg 1995, Heywang-Köbrunner, Bick 2001, Lee, Dershaw 2010, Mintun, Welch 1988, Olsen and Gøtzsche 2001, Weinreb and Newstead 1995, Yang, Le-Petross 2008). Currently, mammography (Nyström, Wall 1993, Olsen and Gøtzsche 2001, Urbain 2005), ultrasound (US) (Gordon and Goldenberg 1995, Jackson 1990, Moon, Myung 2002, Moore and Copel 2011, Yang, Suen 1997), and magnetic resonance imaging (MRI) (Boetes and Stoutjesdijk 2001, Orel and Schnall 2001) are the imaging modalities most frequently utilized in clinical practice. While these diagnostic tools have significantly improved the detection rate of breast cancer and provide invaluable guidance for purposes of management, they have certain limitations. Mammography has limited sensitivity, especially in patients with dense breasts (Berg, Zhang 2012, Carney, Miglioretti 2003, Urbain 2005). Breast US is an invaluable complimentary tool for both detection and characterization of breast cancer (Cole-Beuglet, Soriano 1983, Fornage, Toubas 1987, Ikedo, Fukuoka 2007, Kapur, Carson 2004, Teh and Wilson 1998, Wilkinson, Given-Wilson 2005). However, the use of US imaging of the breast in screening of asymptomatic women is associated with high rates of both false-negative and false-positive results (Berg, Blume 2008, Berg, Zhang 2012, Gartlehner, Thaler 2013, Kolb, Lichy 2002, Sehgal, Weinstein 2006, Teh and Wilson 1998). MRI is expensive and not widely available to all patients. Moreover, breast MRI suffers from low specificity, which leads to unnecessary biopsies (Kriege, Brekelmans 2004, Morris 2001). To overcome these limitations and to enhance the sensitivity and specificity of breast cancer imaging, researchers have examined the utility of new imaging techniques such as elastography (Garra, Cespedes 1997, Plewes, Bishop 2000, Sharma, Soo 2004, Tanter, Bercoff 2008, Zhi, Ou 2007), photoacoustic imaging (Manohar, Kharine 2005) and diffuse optical tomography (Ntziachristos and Chance 2000). Specifically, US-based elastography methods such as quasi-static elastography (REF), supersonic imaging (REF), and acoustic radiation force imaging (ARFI) have shown promising potential in improving the specificity of breast cancer imaging. Our group has introduced vibro-acoustography (VA) as a complimentary technique to improve sensitivity and specificity in clinical breast imaging (Alizad, Fatemi 2004, Alizad, Whaley 2005, Alizad, Whaley 2006, Alizad, Whaley 2008, Alizad, Whaley 2006, Alizad, Whaley 2012, Fatemi, Wold 2002).

In VA, ultrasound is employed to produce a localized low-frequency acoustic radiation force (ARF) to vibrate the tissue. The low-frequency ARF is generated through interaction of two confocal ultrasound beams that are at slightly different frequencies (Fatemi and Greenleaf 1998, Fatemi and Greenleaf 1999). As a result of such interaction, a localized oscillatory

ARF is generated, at a frequency that is equal to the difference between the frequencies of the two primary ultrasound beams, within the small focal region. Upon stimulating the tissue with the ARF, the local vibration of tissue produces acoustic waves that convey information about the acoustical and mechanical properties of the stimulated spot. These acoustic waves are detected by a hydrophone. The process is repeated point-by-point through the entire region of interest while the detected acoustic waves are recorded. Finally, the amplitude of the recorded signal is used to produce an image that represents the distribution of the acoustical and mechanical properties of the object (Fatemi and Greenleaf 1998, Fatemi and Greenleaf 1999, Fatemi and Greenleaf 2000, Fatemi, Manduca 2003). A comprehensive review of VA and its application in medicine are described elsewhere (Urban, Alizad 2011). Although in many VA applications ARF was produced by a dual-element transducer in confocal configuration, several other configurations have also been studied including x-focal using two single element US transducers (Chen, Fatemi 2004), sector array (Silva, Chen 2005), multi-frequency array (Urban, Silva 2006), and linear array (Silva, Greenleaf 2004, Urban, Chalek 2011).

In a previous study (Alizad, Whaley 2012, Fatemi, Wold 2002), we used a confocal VA system to demonstrate the capability of VA in detection of various breast abnormalities, including microcalcifications as well as benign and malignant masses with relatively high specificity (Alizad, Whaley 2012). In this VA system, a large-size fixed focus two-element confocal transducer was used to generate the ARF, and the VA images were acquired by mechanically scanning across the object. This system was equipped with a water tank to accommodate acoustic coupling to tissue while scanning the object in raster motion. A drawback of this system was limited access to parts of the breast near the chest wall. Also, the need for two-dimensional raster scanning of the transducer resulted in slow image acquisition.

To overcome the limitations of the prototype confocal VA system and pave the way for clinical use of VA, we redesigned the system by implementing VA functionality on a clinical ultrasound imaging system and employed a Q2D array ultrasound transducer, consisting of a matrix of 12 rows by 70 columns of ultrasound elements, with electronic scanning capability (Urban, Chalek 2013, Urban, Fatemi 2010). Here, we present the preliminary *in vivo* results of breast VA obtained by the new VA system equipped with a Q2D array transducer. To the best of our knowledge, the present report is the first demonstration of VA implemented on a quasi-2D US transducer to image breast lesions in human subjects.

## Methods

### Development of a Q2DVA system

In the confocal VA system, a fixed focus confocal US transducer, comprising of two piezoelectric elements in the shape of a center disk surrounded by a ring-shaped piezoelectric was used to remotely vibrate the tissue at a low frequency. Additional technical details of the confocal VA system are described elsewhere (Alizad, Whaley 2012, Fatemi, Wold 2002). While the results obtained from the confocal VA system are promising and indicate the ability of VA to detect and characterize the breast lesions (Alizad, Whaley

2012), the use of such system for clinical application is associated with some difficulties. Long scanning time and the discomfort associated with prone patient positioning are examples of such difficulties. Moreover, the confocal VA probe must mechanically move in a small water tank to raster scan the breast. In the confocal VA system, a small water tank had an acoustically transparent side window covered by a thin membrane of 80×120 mm, made out of tapered latex-free transducer cover (CIV-Flex, Civco Medical Solutions, Iowa, USA). The breast was placed outside the water tank in contact with the membrane. The ultrasound beam passed through the window into the breast to scan the beast in the cranial-caudal plane in a prone position. In this arrangement, the size of the water tank and the transducer limited access to the upper parts of the breast and close to the chest wall; thus, lesions in these locations could not be covered within the VA image frame. This latter limitation could significantly constrain the applicability of confocal VA for clinical practice, because the majority of the malignant lesions develop in the upper outer quadrant (43%) and upper inner quadrant (22%) (Cao 2009, Darbre 2005, Moore, Dalley 2013).

To address the limitations of the confocal VA system and as a step towards development of a clinical VA breast scanner, VA has been implemented on a clinical ultrasound scanner (GE Vivid 7, GE Healthcare Ultrasound Cardiology, Horten, Norway) equipped with a "Q2D" ultrasound transducer. The Q2D transducer array is in the form of a matrix with multiple rows and columns of ultrasound elements (Urban, Chalek 2013) that can be electronically configured to optimally generate an ultrasound beam that resembles that of the confocal transducer.

The block diagram of the Q2DVA system is shown in **Fig. 1a**. A clinical US scanner (GE Vivid 7) was modified to perform VA imaging in addition to conventional B-scan US and VA imaging. The modified system was able to transmit ultrasound beams at two different frequencies and generate the low-frequency ARF required for VA. The scanner drives a Q2D array US transducer, designed by GE and manufactured by Tetrad, a subsidiary of W. L. Gore (Englewood, CO). The Q2D array US transducer consisted of 840 piezoelectric elements in the form of a matrix of 70 columns by 12 rows (**Fig. 1b**). Each piezoelectric element size was 900 by 900 μm. The Q2D array US transducer was designed for the operating frequencies between 5 to 8 MHz. Since the ultrasound scanner was capable of simultaneously driving 128 channels, a subset of the 12 by 12 elements were selected to form an "active" VA aperture (Urban, Chalek 2013) (**Fig. 1c**). Out of the 144 elements within the selected square sub-aperture, 128 elements could be active at a time (i.e. driven by GE vivid 7 scanner). In our VA studies, the active aperture is divided into an exterior ring-shaped section (elements marked with red color) around a center square shaped section (elements marked with green color). The black-colored elements are inactive elements in this sub-aperture configuration. This configuration, which we have termed "null-corner-center", can closely approximate a dual-element confocal transducer where a ring-shaped piezoelectric crystal surrounds a center disk (Fatemi and Greenleaf 1998, Fatemi and Greenleaf 1999). In the case shown in **Fig. 1c**, the ring-shaped section, marked in red, transmits the acoustic waves at $f_1$ = 4.9485 MHz and the central portion (green) transmits at $f_2$ = 5.000 MHz. These two beams intersect and generate a low frequency modulated ARF at the difference frequency of $\Delta f$ = 51.5 kHz at the focal region. A needle hydrophone

(HGL-0200, Onda Corp., Sunnyvale, CA) having an active element with 0.200 mm diameter and a 20-dB preamplifier (AH- 2000, Onda Corp.) was utilized to scan the acoustic field in both azimuthal-axial (XZ) and focal (XY or C-) planes. To demonstrate the spatial distribution of the low-frequency ARF, the normalized intensities of ARF in azimuthal direction (X), elevation direction (Y), and axial direction (Z) are shown in **Figure 2**. **Figure 2a** demonstrates the azimuthal and elevation distribution of the ARF on a focal plane and indicates the symmetry of the ARF on the focal plane. **Figure 2b** shows the axial distribution of the ARF when the focal depth is set at 25 mm. Further details of the described configuration are studied by Urban et. al. (Urban, Chalek 2013). The mechanical index (MI) was measured as 0.329, lower than the safety requirement of 1.9. This indicates that the developed VA system operates far below safety requirements of US intensity/ pressure for the safe use of diagnostic US in medicine (Barnett, Ter Haar 2000). The spatial peak-temporal average intensity ($I_{SPTA}$) for the null-center-corner configuration was measured as 14 $mW/cm^2$ which is significantly lower than FDA requirement (720 $mW/cm^2$). Upon applying the localized ARF, the acoustic emission due to the tissue vibrations was detected by a pre-amplified hydrophone (B&K-8106 C; Bruel & Kjaer, Denmark) placed on the breast near the probe (**Fig. 1a**). The signals detected by the hydrophone were filtered by a bandpass (BP) filter (40-60 KHz bandwidth) and then digitized. The digitized signal was sampled at 5 Ms/s and was stored in a computer for VA image reconstruction and further post-processing. The mean of the recorded signal was subtracted from the signal to remove the DC bias. The amplitude (rms) of the recorded acoustic signal was used to reconstruct the VA images. Since the signal acquisition is longer than an actual acoustic emission due to VA excitation, time-gating was performed to time filter the signal that conveys the VA information. A 5×5 2-D mean filter was applied on reconstructed images to further remove the noises.

During scanning, a digitally controlled multiplexer is utilized to electronically translate and steer the active aperture along the azimuthal direction and over the total aperture of the transducer. The probe is moved in the perpendicular (elevation) direction by a motorized linear axis (not shown in **Fig. 1a**) to mechanically scan the tissue (with the step size of 200 μm) and provide C-plane VA images (C-plane is the plane parallel to the face of the Q2D transducer). By focusing the beams at the desired depths, several equally distanced parallel imaging C-planes are scanned at various depths ranging from 15 to 40 mm (depending on size and location of the lesions) and in 2.5 mm steps in the depth direction.

### *In vivo* patient study

Prior to *in vivo* patient studies, the Q2DVA system was optimized by selecting the US beams' configuration, placement of the hydrophone, and a scanning speed that provided the best results. By utilizing Q2D transducer, it is possible to set different configurations for probe elements to transmit $f_1$ and $f_2$, and thus, generate low frequency ARF with different spatial distribution (Urban, Chalek 2013). Upon testing a number of different configurations, the null-corner-center configuration (**Fig. 1c**) was selected due to the higher quality of VA images. The selected US beams' configuration for generating ARF allows for generating a symmetric ARF with smaller side lobes, which is a necessity to provide better quality VA images. The hydrophone was placed on the breast near the Q2DVA probe, but not touching

it. Depending on lesion location and breast size, the hydrophone was placed mediolaterally above the probe in most cases, and in some cases, lateral to the breast. A delay of 500 ms between each scanning line was also found to enhance the Q2DVA images by allowing the probe to settle during the mechanical scanning. The optimization was performed only once and the optimized settings were utilized for the entire *in vivo* study. To evaluate the performance of the VA system with a Q2D array transducer in a clinical setting, we utilized this system to characterize breast lesions in several patients prior to percutaneous core needle biopsy. Patients selected for evaluation were noted to have a suspicious finding in one or both breasts demonstrated with conventional breast imaging techniques. All *in vivo* imaging procedures were performed according to a protocol approved by the Mayo Clinic Institutional Review Board. Informed consents were obtained prior to imaging. Biopsy of suspicious breast lesions occurred after imaging with the VA system in all cases.

Patients were scanned in the supine position, similar to the position commonly used in clinical practice of conventional breast US (Jackson 1990, Madjar and Mendelson 2008). The Q2D probe was placed on the breast with suspicious findings and ultrasound gel was used for coupling. A series of B-mode US images were acquired using the same Q2D US transducer prior to VA imaging. Upon locating the suspicious breast lesion, the region of interest and the depth of the lesions were determined for VA scans. The motorized axis positioned the Q2D probe to the location where the VA scans start. Several C-planes at various depths ranging from 15 to 40 mm (depending on the size of the breast and the location of the lesion) were scanned by changing the focus of the US beams (Urban, Fatemi 2010). A custom-built LabVIEW® (National Instruments, Texas, USA) application was developed to control the ultrasound scanner, motorized axis, and the data acquisition systems to perform the VA scans. The current imaging system is configured to utilize tonebursts of 333 μs to generate the ARF. However, there is a delay between applying consecutive tonebursts to avoid overheating the hardware and the Q2DVA probe. In electronic beam scanning, the time required to excite and detect the signal from each pixel is set to 2 ms. Besides, there is a 500 ms delay between each motor movement (i.e. mechanical scan). Most images have 192 pixels in the electronic scanning direction (i.e. per line) and the images consist of 265 lines. Therefore, the scan time per C-plane image was about 221 seconds.

## Results

Here, we present the VA images of six selected cases to demonstrate the ability of this system to detect and localize different types of breast lesions. Amongst the selected 6 cases, three were benign and three were malignant. To further support our VA results and provide correlation with conventional imaging, select mammographic views and targeted clinical US images of each case are included. Biopsy results of each case are also reported for clinical correlation. It must be noted that this study was a preliminary feasibility study to evaluate the ability of Q2DVA in breast imaging. Therefore, we did not intend to statistically evaluate the sensitivity or specificity of Q2DVA in classifying different types of breast lesions.

### Case 1: Invasive ductal carcinoma

A woman in her 50s presented for breast imaging evaluation with a palpable lump in her right breast. Her mammogram (**Fig. 3a**) revealed a heterogeneous dense breast with a central focal asymmetry corresponding to the region of palpable concern (marked with a dashed yellow contour). The mammogram indicates the presence of small microcalcifications (marked with red arrows). Targeted clinical US (**Fig. 3b**) confirmed the presence of a 21 mm ×14 mm irregular hypoechoic mass (measured 2.34 in the azimuthal direction) with an indistinct margin and posterior acoustic shadowing, corresponding to the mammographic asymmetry. VA images obtained with the Q2D probe and at depths of 25 and 27.5 mm clearly show the mass at both imaging depths (**Fig. 3c** and **3d)**. It is worth reiterating that in all cases, the VA image plane is perpendicular to that of B-mode US. The dimensions of the lesions at both depths are larger than those of the clinical US image. Similar findings have been seen and confirmed in our previous VA study (Alizad, Whaley 2012), where malignant breast lesions appeared larger in VA than in B-mode US. The VA image obtained at the depth of 25 mm depicts the presence of small calcifications within the mass marked by red arrows (**Fig. 3c**). Whereas the depth of the mass is determined to be between 10 to 25 mm in US B-scans, the mass appears deeper on VA images (i.e. 25 and 27.5 mm). This discrepancy in depth is thought to relate to mild transducer compression during B-mode US imaging, which did not occur during Q2DVA imaging. The lesion is visualized with a lower contrast at 27.5 mm depth (**Fig. 3d**) indicating the deeper boundary of the lesion is located approximately at 27.5 mm. Percutaneous core needle biopsy of this mass performed under US guidance demonstrated invasive ductal carcinoma, Nottingham grade II.

### Case 2: Benign fibroadenoma

A woman in her 30s presented with palpable concern in her left breast. Diagnostic mammography (**Fig. 4a**) revealed heterogeneously dense breast parenchyma and a small mass (marked with a yellow arrow) in the anterior depth of the left breast with mostly circumscribed margins. Clinical US of the left breast demonstrated a corresponding 14 × 6 mm hypoechoic solid mass with circumscribed margins in parallel orientation (**Fig. 4b**). VA images of the left breast obtained with Q2D probe at various depths between 17.5 to 22.5 mm reveal the presence of the mass in all depths (**Fig. 4c**-**4e**). The size of the visualized lesion estimated by VA imaging is in complete agreement with clinical US findings. US guided percutaneous core needle biopsy of this mass revealed a benign fibroadenoma.

### Case 3: Fibroadenoma

A woman in her 40s presented with a palpable lump in her left breast. Diagnostic mammography (**Fig. 5a**) showed a heterogeneous dense breast and a 15 mm well-circumscribed solid mass at the anterior depth (marked with a yellow arrow). The bright triangle marked with a red arrow represents the triangular skin marker. Her targeted clinical US (**Fig. 5b**) revealed a corresponding solid round mass with circumscribed margins. VA images obtained at a depth of 20 mm (**Fig. 5c**) reveal a corresponding mass with a well-defined margin (marked with yellow arrows). US guided biopsy revealed a benign fibroadenoma.

### Case 4: Sclerosing fibroadenoma

A woman in her 50s presented with an abnormality noted on annual screening. Diagnostic mammogram (**Fig. 6a**) demonstrates an oval mass with partially obscured margins in the posterior depth of the right breast (marked with a yellow arrow). Due to the shape of this lesion, measurements were somewhat difficult. A targeted transverse US image (**Fig. 6b**) shows a corresponding oval hypoechoic mass with posterior shadowing that measured 19 × 10 × 10 mm. The VA image obtained at a depth of 30 mm (**Fig. 6c)** shows an elongated mass with a well-defined border suggesting a benign lesion. Percutaneous biopsy with ultrasound guidance revealed a sclerosing fibroadenoma with densely hyalinized stroma with occasional duct epithelial spaces. The sclerosing accounts for the shadowing posterior to the lesion. The mass is well-visualized (dark) in the VA image. Visualization of the lesion at deeper depths by VA than what was shown in B-mode imaging is due to transducer compression of the breast tissue during the clinical US imaging procedure.

### Case 5: Invasive ductal carcinoma

A woman in her 60s presented for diagnostic imaging evaluation of her right breast. Diagnostic mammography (**Fig. 7a**) of the right breast demonstrates scattered fibroglandular densities with a possible asymmetry at middle depth (marked with a dashed yellow contour). Targeted US demonstrates a 12 × 10 × 10 mm irregular hypoechoic mass with ill-defined margins and posterior shadowing (**Fig. 7b**). The VA images at 25 mm and 27.5 mm depths of the same breast (**Fig. 7c** and **7d**, respectively) identify the mass with its irregular marginal extension marked with red arrows. US guided biopsy revealed infiltrating ductal carcinoma, Nottingham grade I (of III).

### Case 6: Invasive ductal carcinoma

A woman in her 70s presented with a palpable lump in her right breast. Diagnostic mammogram (**Fig. 8a**) demonstrated a focal asymmetry in the anterior depth breast corresponding to the area of concern. Targeted US (**Fig. 8b**) shows a corresponding irregular shaped hypoechoic mass that measures 13 × 12 × 8 mm. Q2DVA performed at 17.5 mm depth (**Fig. 8c**) further documents this mass with suspicious features. Similar to Case 1, the lesions appeared lager in VA than in B-mode US. US guided biopsy confirmed invasive ductal carcinoma.

## Discussion

The objective of this study was to investigate the feasibility of VA with a Q2D US probe for breast cancer imaging. Although our previous study utilizing prone confocal VA showed promising results (Alizad, Whaley 2012), the utility of confocal VA for breast imaging has two major limitations: problem accessing parts of breast near the chest wall due to the use of a water tank and lengthy scanning time. The Q2DVA system with the probe can overcome these limitations. The Q2D probe can easily reach almost any part of the breast similar to conventional breast US. Imaging time with the newly designed VA system is reduced by approximately 66% compared to the time needed for imaging with the confocal VA system. The main reason is that the confocal VA requires mechanical scanning in two directions, whereas Q2DVA requires only one directional mechanical scanning. The scanning time can

be further shortened by using a full 2D array US transducer that enables fully electronically scanning the whole C-plane with no need for mechanical scanning.

A key advantage of the Q2DVA system is that it can be easily combined with a clinical US imaging system with no need for any complex hardware modifications to provide more information for clinicians. VA images convey information about both mechanical and acoustic properties of the tissue. In other words, VA can provide clinically-relevant information about the lesions beyond what is acquired by B-mode US imaging. The speckle-free nature of VA images makes it easier to observe the abnormalities compared to typical conventional B-mode image.

The VA images represented in the results section are simply reconstructed from the amplitude of the acoustic emission; additional signal and image processing algorithms were not required. The resolution of the Q2DVA images is determined by the spatial distribution of the ARF and is in the millimeter range. Such resolution is generally sufficient for detecting the breast lesions. The Q2D probe provides an almost symmetric distribution of ARF, similar to that of the confocal VA system. Therefore, the quality of acquired VA images is comparable to the ones obtained by using the confocal VA probe. In comparison with confocal breast VA, there were a few difficulties in the performance of *in vivo* image acquisition with the Q2DVA system. First, system artifact associated with steering the VA beams across the aperture resulted in mild streak-type artifacts in the acquired images. We have developed an algorithm to correct for these artifacts (Urban, Chalek 2011). In addition, during *in vivo* scanning with the Q2DVA system, breathing motion introduced undesired artifacts in VA images. Such artifacts can be seen in Figures **3c-3e**, appearing as jagged edges on the image. Continued development of VA in terms of hardware improvement and signal processing can potentially eliminate such artifacts and enhance the quality of VA images and eventually lead to an imaging modality with higher sensitivity and specificity.

The results shown in this report suggest the feasibility of clinical implementation of VA by using a Q2D probe. Further studies are required to evaluate the sensitivity and specificity of Q2DVA in imaging breast cancer. We speculate that using a full 2D US transducer can further enhance the VA images and make it more suitable for clinical usage. Since VA and US share common hardware (US scanner and transducer), we envision that in the future VA can be combined with conventional US imaging and become a hybrid imaging modality that can provide physicians with further clinically useful information.

## Conclusions

We have investigated the feasibility of using VA with a Q2D array US transducer for detection and localization of breast lesions. The work presented in this study is built upon our previous studies in which confocal VA was introduced as a high sensitivity and specificity tool for breast cancer imaging. The results represented in this report demonstrate that VA implemented on a clinical ultrasound scanner equipped with a Q2D US transducer can detect and localize breast lesions. The Q2DVA system can eliminate practical difficulties associated with using confocal VA, such as the inability to image the lesions close to the chest wall, and the discomfort associated with patient positioning and breast

compression. Our results should provide a foundation for further development of clinical VA systems and further investigation in a larger group of patients.

## Acknowledgements

This study was supported by NIH Grants R21CA121579, R01CA148994 and R01CA127235 from the National Institute of Health. The authors are grateful to Dr. James F. Greenleaf and Dr. Matthew W. Urban for their helpful discussions, to Thomas Kinter for computer support, and to Jennifer Milliken for administrative support.

## References

Adler DD, Carson PL, Rubin JM, Quinn-Reid D. Doppler ultrasound color flow imaging in the study of breast cancer: preliminary findings. Ultrasound in medicine & biology. 1990; 16:553–59. [PubMed: 2238263]

Alizad A, Fatemi M, Wold LE, Greenleaf JF. Performance of vibro-acoustography in detecting microcalcifications in excised human breast tissue: A study of 74 tissue samples. Medical Imaging, IEEE Transactions on. 2004; 23:307–12.

Alizad A, Whaley D, Greenleaf J, Fatemi M. Potential applications of vibro-acoustography in breast imaging. Technology in cancer research & treatment. 2005; 4:151. [PubMed: 15773784]

Alizad A, Whaley DH, Greenleaf JF, Fatemi M. Critical issues in breast imaging by vibro-acoustography. Ultrasonics. 2006; 44:e217–e20. [PubMed: 16843513]

Alizad A, Whaley DH, Greenleaf JF, Fatemi M. Image features in medical vibro-acoustography: In vitro and in vivo results. Ultrasonics. 2008; 48:559–62. [PubMed: 18599102]

Alizad A, Whaley DH, Kinnick RR, Greenleaf JF, Fatemi M. P2E-1 In Vivo Breast Vibro-Acoustography: Recent Results and New Challenges. *Ultrasonics Symposium, 2006. IEEE*: IEEE. 2006:1659–62.

Alizad A, Whaley DH, Urban MW, Carter RE, Kinnick RR, Greenleaf JF, Fatemi M. Breast vibro-acoustography: initial results show promise. Breast Cancer Research. 2012; 14:R128. [PubMed: 23021305]

Barnett SB, Ter Haar GR, Ziskin MC, Rott H-D, Duck FA, Maeda K. International recommendations and guidelines for the safe use of diagnostic ultrasound in medicine. Ultrasound in medicine & biology. 2000; 26:355–66. [PubMed: 10773365]

Berg WA, Blume JD, Cormack JB, Mendelson EB, Lehrer D, Böhm-Vélez M, Pisano ED, Jong RA, Evans WP, Morton MJ. Combined screening with ultrasound and mammography vs mammography alone in women at elevated risk of breast cancer. JAMA: the journal of the American Medical Association. 2008; 299:2151–63.

Berg WA, Zhang Z, Lehrer D, Jong RA, Pisano ED, Barr RG, Böhm-Vélez M, Mahoney MC, Evans WP III, Larsen LH. Detection of breast cancer with addition of annual screening ultrasound or a single screening MRI to mammography in women with elevated breast cancer risk. JAMA: the journal of the American Medical Association. 2012; 307:1394–404.

Bluemke DA, Gatsonis CA, Chen MH, DeAngelis GA, DeBruhl N, Harms S, Heywang-Köbrunner SH, Hylton N, Kuhl CK, Lehman C. Magnetic resonance imaging of the breast prior to biopsy. JAMA: the journal of the American Medical Association. 2004; 292:2735–42.

Boetes C, Stoutjesdijk M. MR imaging in screening women at increased risk for breast cancer. Magnetic resonance imaging clinics of North America. 2001; 9:357. [PubMed: 11493425]

Cao Z. Mammographic features of breast cancer: Analysis of 118 cases. The Chinese-German Journal of Clinical Oncology. 2009; 8:659–64.

Carney PA, Miglioretti DL, Yankaskas BC, Kerlikowske K, Rosenberg R, Rutter CM, Geller BM, Abraham LA, Taplin SH, Dignan M. Individual and combined effects of age, breast density, and hormone replacement therapy use on the accuracy of screening mammography. Annals of Internal Medicine. 2003; 138:168–75. [PubMed: 12558355]

Chen S, Fatemi M, Kinnick R, Greenleaf JF. Comparison of stress field forming methods for vibro acoustography. Ultrasonics, Ferroelectrics and Frequency Control, IEEE Transactions on. 2004; 51:313–21.

Cole-Beuglet C, Soriano R, Kurtz A, Goldberg B. Ultrasound analysis of 104 primary breast carcinomas classified according to histopathologic type. Radiology. 1983; 147:191–96. [PubMed: 6828727]

Corsetti V, Houssami N, Ghirardi M, Ferrari A, Speziani M, Bellarosa S, Remida G, Gasparotti C, Galligioni E, Ciatto S. Evidence of the effect of adjunct ultrasound screening in women with mammography-negative dense breasts: Interval breast cancers at 1year follow-up. European Journal of Cancer. 2011; 47:1021–26. [PubMed: 21211962]

Darbre PD. Recorded quadrant incidence of female breast cancer in Great Britain suggests a disproportionate increase in the upper outer quadrant of the breast. Anticancer research. 2005; 25:2543–50. [PubMed: 16080490]

Fatemi M, Greenleaf JF. Ultrasound-stimulated vibro-acoustic spectrography. Science. 1998; 280:82–85. [PubMed: 9525861]

Fatemi M, Greenleaf JF. Vibro-acoustography: An imaging modality based on ultrasound-stimulated acoustic emission. Proceedings of the National Academy of Sciences. 1999; 96:6603–08.

Fatemi M, Greenleaf JF. Probing the dynamics of tissue at low frequencies with the radiation force of ultrasound. Physics in medicine and biology. 2000; 45:1449. [PubMed: 10870703]

Fatemi M, Manduca A, Greenleaf JF. Imaging elastic properties of biological tissues by low-frequency harmonic vibration. Proceedings of the IEEE. 2003; 91:1503–19.

Fatemi M, Wold LE, Alizad A, Greenleaf JF. Vibro-acoustic tissue mammography. Medical Imaging, IEEE Transactions on. 2002; 21:1–8.

Fornage BD, Toubas O, Morel M. Clinical, mammographic, and sonographic determination of preoperative breast cancer size. Cancer. 1987; 60:765–71. [PubMed: 3297295]

Garra BS, Cespedes EI, Ophir J, Spratt SR, Zuurbier RA, Magnant CM, Pennanen MF. Elastography of breast lesions: initial clinical results. Radiology. 1997; 202:79–86. [PubMed: 8988195]

Gartlehner G, Thaler K, Chapman A, Kaminski-Hartenthaler A, Berzaczy D, Van Noord MG, Helbich TH. Mammography in combination with breast ultrasonography versus mammography for breast cancer screening in women at average risk. Cochrane Database Syst Rev. 2013; 4

Gordon PB, Goldenberg SL. Malignant breast masses detected only by ultrasound. A retrospective review. Cancer. 1995; 76:626–30. [PubMed: 8625156]

Heywang-Köbrunner S, Bick U, Bradley W Jr, Bone B, Casselman J, Coulthard A, Fischer U, Müller-Schimpfle M, Oellinger H, Patt R. International investigation of breast MRI: results of a multicentre study (11 sites) concerning diagnostic parameters for contrast-enhanced MRI based on 519 histopathologically correlated lesions. European radiology. 2001; 11:531–46. [PubMed: 11354744]

Ikedo Y, Fukuoka D, Hara T, Fujita H, Takada E, Endo T, Morita T. Development of a fully automatic scheme for detection of masses in whole breast ultrasound images. Medical Physics. 2007; 34:4378. [PubMed: 18072503]

Jackson VP. The role of US in breast imaging. Radiology. 1990; 177:305–11. [PubMed: 2217759]

Kapur A, Carson PL, Eberhard J, Goodsitt MM, Thomenius K, Lokhandwalla M, Buckley D, Roubidoux MA, Helvie MA, Booi RC. Combination of digital mammography with semi-automated 3D breast ultrasound. Technology in cancer research & treatment. 2004; 3:325. [PubMed: 15270583]

Kolb TM, Lichy J, Newhouse JH. Comparison of the performance of screening mammography, physical examination, and breast us and evaluation of factors that influence them: an analysis of 27,825 patient evaluations1. Radiology. 2002; 225:165–75. [PubMed: 12355001]

Kriege M, Brekelmans CT, Boetes C, Besnard PE, Zonderland HM, Obdeijn IM, Manoliu RA, Kok T, Peterse H, Tilanus-Linthorst MM. Efficacy of MRI and mammography for breast-cancer screening in women with a familial or genetic predisposition. New England Journal of Medicine. 2004; 351:427–37. [PubMed: 15282350]

Lee CH, Dershaw DD, Kopans D, Evans P, Monsees B, Monticciolo D, Brenner RJ, Bassett L, Berg W, Feig S. Breast cancer screening with imaging: recommendations from the Society of Breast Imaging and the ACR on the use of mammography, breast MRI, breast ultrasound, and other technologies for the detection of clinically occult breast cancer. Journal of the American College of Radiology. 2010; 7:18–27. [PubMed: 20129267]

Madjar, H.; Mendelson, E. The practice of breast ultrasound: techniques, findings, differential diagnosis: Thieme. 2008.

Manohar S, Kharine A, van Hespen JC, Steenbergen W, van Leeuwen TG. The Twente Photoacoustic Mammoscope: system overview and performance. Physics in medicine and biology. 2005; 50:2543. [PubMed: 15901953]

Mintun M, Welch M, Siegel B, Mathias C, Brodack J, McGuire A, Katzenellenbogen J. Breast cancer: PET imaging of estrogen receptors. Radiology. 1988; 169:45–48. [PubMed: 3262228]

Moon WK, Myung JS, Lee YJ, Park IA, Noh D-Y, Im J-G. US of Ductal Carcinoma In Situ1. Radiographics. 2002; 22:269–81. [PubMed: 11896217]

Moore CL, Copel JA. Point-of-care ultrasonography. New England Journal of Medicine. 2011; 364:749–57. [PubMed: 21345104]

Moore, KL.; Dalley, AF.; Agur, AM. Clinically oriented anatomy: Wolters Kluwer Health. 2013.

Morris EA. Review of breast MRI: indications and limitations. *Seminars in roentgenology*: WB Saunders. 2001:226–37.

Ntziachristos V, Chance B. Breast imaging technology: Probing physiology and molecular function using optical imaging-applications to breast cancer. Breast Cancer Research. 2000; 3:41. [PubMed: 11250744]

Nyström L, Wall S, Rutqvist L, Lindgren A, Lindqvist M, Ryden S, Andersson J, Bjurstam N, Fagerberg G, Frisell J. Breast cancer screening with mammography: overview of Swedish randomised trials. The Lancet. 1993; 341:973–78.

Olsen O, Gøtzsche PC. Cochrane review on screening for breast cancer with mammography. The Lancet. 2001; 358:1340–42.

Orel SG, Schnall MD. MR Imaging of the Breast for the Detection, Diagnosis, and Staging of Breast Cancer1. Radiology. 2001; 220:13–30. [PubMed: 11425968]

Plewes DB, Bishop J, Samani A, Sciarretta J. Visualization and quantification of breast cancer biomechanical properties with magnetic resonance elastography. Physics in medicine and biology. 2000; 45:1591. [PubMed: 10870713]

Sehgal CM, Weinstein SP, Arger PH, Conant EF. A review of breast ultrasound. Journal of mammary gland biology and neoplasia. 2006; 11:113–23. [PubMed: 17082996]

Sharma AC, Soo MS, Trahey GE, Nightingale KR. Acoustic radiation force impulse imaging of in vivo breast masses. *Ultrasonics Symposium, 2004 IEEE*: IEEE. 2004:728–31.

Siegel R, Naishadham D, Jemal A. Cancer statistics, 2013. CA: a cancer journal for clinicians. 2013; 63:11–30. [PubMed: 23335087]

Silva GT, Chen S, Frery AC, Greenleaf JF, Fatemi M. Stress field forming of sector array transducers for vibro-acoustography. Ultrasonics, Ferroelectrics and Frequency Control, IEEE Transactions on. 2005; 52:1943–51.

Silva GT, Greenleaf JF, Fatemi M. Linear arrays for vibro-acoustography: a numerical simulation study. Ultrasonic imaging. 2004; 26:1–17. [PubMed: 15134390]

Tanter M, Bercoff J, Athanasiou A, Deffieux T, Gennisson J-L, Montaldo G, Muller M, Tardivon A, Fink M. Quantitative assessment of breast lesion viscoelasticity: initial clinical results using supersonic shear imaging. Ultrasound in medicine & biology. 2008; 34:1373–86. [PubMed: 18395961]

Teh W, Wilson A. The role of ultrasound in breast cancer screening. A consensus statement by the European Group for Breast Cancer Screening. European Journal of Cancer. 1998; 34:449–50. [PubMed: 9713292]

Urbain J-L. Breast cancer screening, diagnostic accuracy and health care policies. Canadian Medical Association Journal. 2005; 172:210–11. [PubMed: 15655243]

Urban MW, Alizad A, Aquino W, Greenleaf JF, Fatemi M. A Review of Vibro-acoustography and its Applications in Medicine. Current medical imaging reviews. 2011; 7:350. [PubMed: 22423235]

Urban MW, Chalek C, Haider B, Thomenius KE, Fatemi M, Alizad A. A beamforming study for implementation of vibro-acoustography with a 1.75-D array transducer. Ultrasonics, Ferroelectrics and Frequency Control, IEEE Transactions on. 2013; 60:535–51.

Urban MW, Chalek C, Kinnick RR, Kinter TM, Haider B, Greenleaf JF, Thomenius KE, Fatemi M. Implementation of vibro-acoustography on a clinical ultrasound system. Ultrasonics, Ferroelectrics and Frequency Control, IEEE Transactions on. 2011; 58:1169–81.

Urban MW, Fatemi M, Alizad A. Beamforming for vibro-acoustography using a 1.75 D array transducer. The Journal of the Acoustical Society of America. 2010; 127:1828–28.

Urban MW, Silva GT, Fatemi M, Greenleaf JF. Multifrequency vibro-acoustography. Medical Imaging, IEEE Transactions on. 2006; 25:1284–95.

Weinreb JC, Newstead G. MR imaging of the breast. Radiology. 1995; 196:593–610. [PubMed: 7644617]

Wilkinson L, Given-Wilson R, Hall T, Potts H, Sharma A, Smith E. Increasing the diagnosis of multifocal primary breast cancer by the use of bilateral whole-breast ultrasound. Clinical radiology. 2005; 60:573–78. [PubMed: 15851045]

Yang W, Suen M, Ahuja A, Metreweli C. In vivo demonstration of microcalcification in breast cancer using high resolution ultrasound. British journal of radiology. 1997; 70:685–90. [PubMed: 9245879]

Yang WT, Le-Petross HT, Macapinlac H, Carkaci S, Gonzalez-Angulo AM, Dawood S, Resetkova E, Hortobagyi GN, Cristofanilli M. Inflammatory breast cancer: PET/CT, MRI, mammography, and sonography findings. Breast cancer research and treatment. 2008; 109:417–26. [PubMed: 17653852]

Zhi H, Ou B, Luo B-M, Feng X, Wen Y-L, Yang H-Y. Comparison of ultrasound elastography, mammography, and sonography in the diagnosis of solid breast lesions. Journal of Ultrasound in Medicine. 2007; 26:807–15. [PubMed: 17526612]

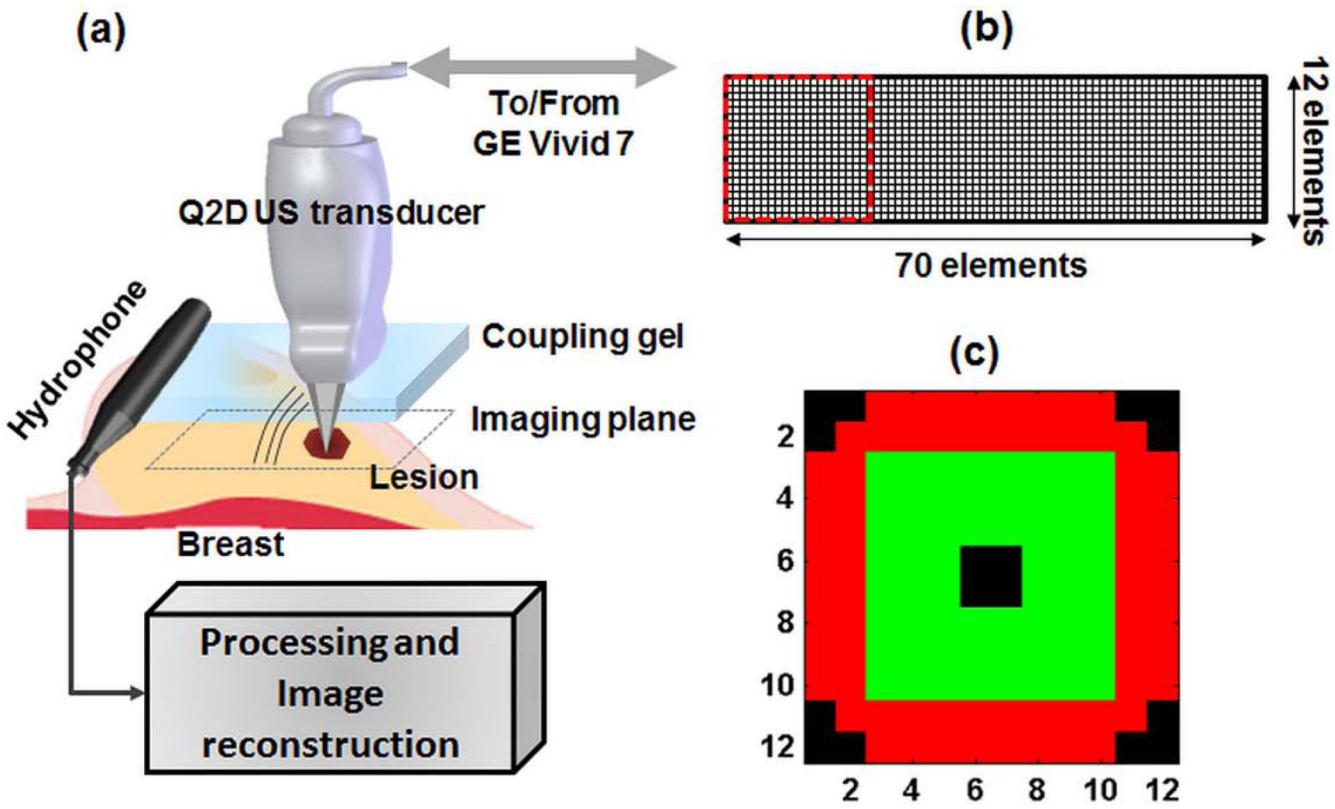


**Figure 1.**

(a). Block diagram of the VA imaging system incorporating a clinical US scanner equipped with a Q2D US transducer. The probe is moved by a motorized axis (not shown in figure) to mechanically scan the imaging plane (C-plane). (b) The element arrangement of the Q2D array US transducer utilizes 12 rows and 70 columns of piezoelectric elements. The active sub-aperture utilizes 144 elements within a square of 12 by 12 elements, marked with the dotted red square. (c) The active sub-aperture element configuration which includes a ring-shaped section, marked in red transmitting the ultrasonic waves at $f_1$, and the central portion (green) that transmits at $f_2$ (null-corner-center).

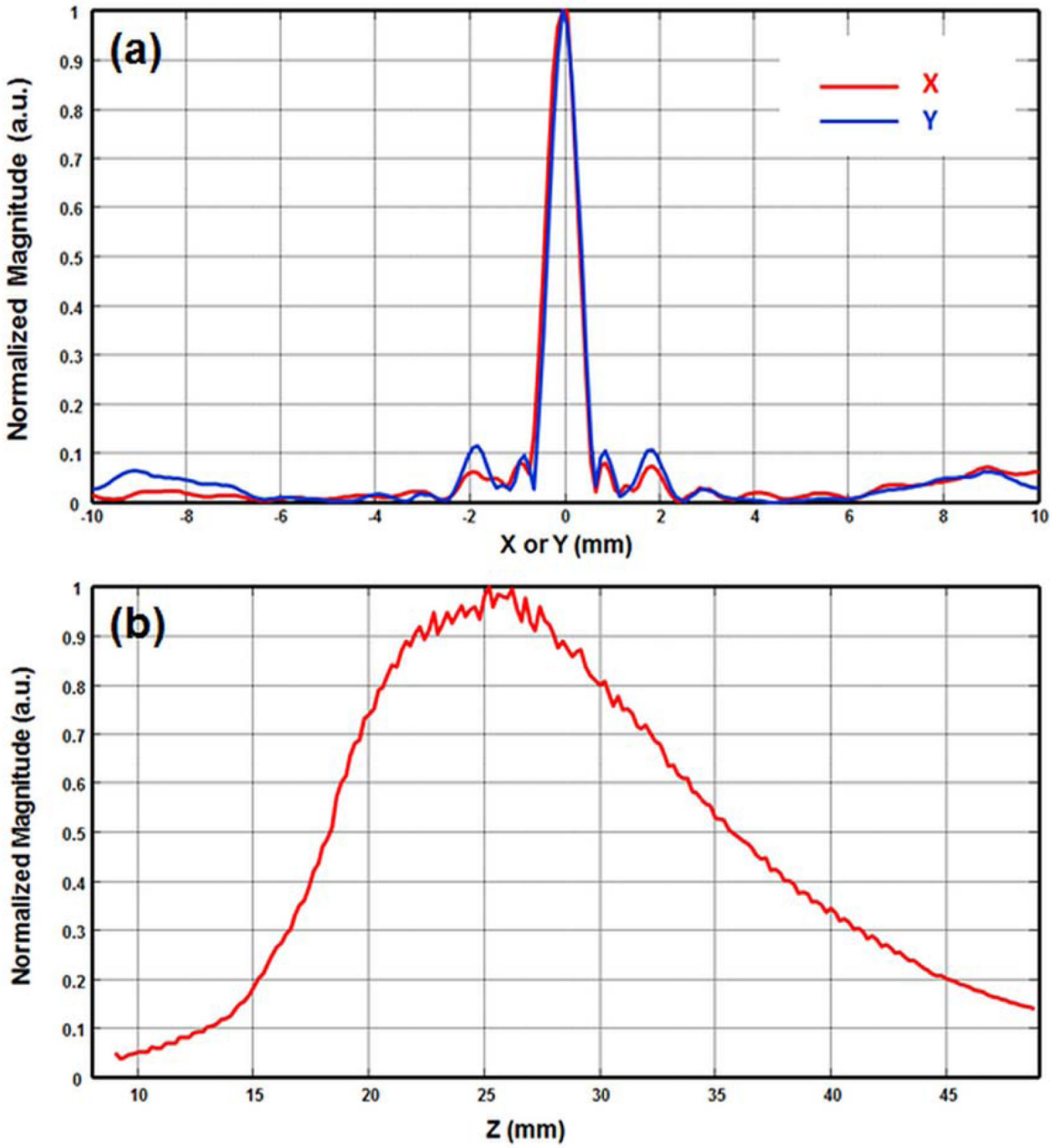


**Figure 2.**

(a) Normalized intensity of ARF on focal plane in azimuthal (X) and elevation (Y) directions (red and blue respectively). (b) Normalized intensity of ARF in axial (Z) direction when the focal depth is set at 25 mm.

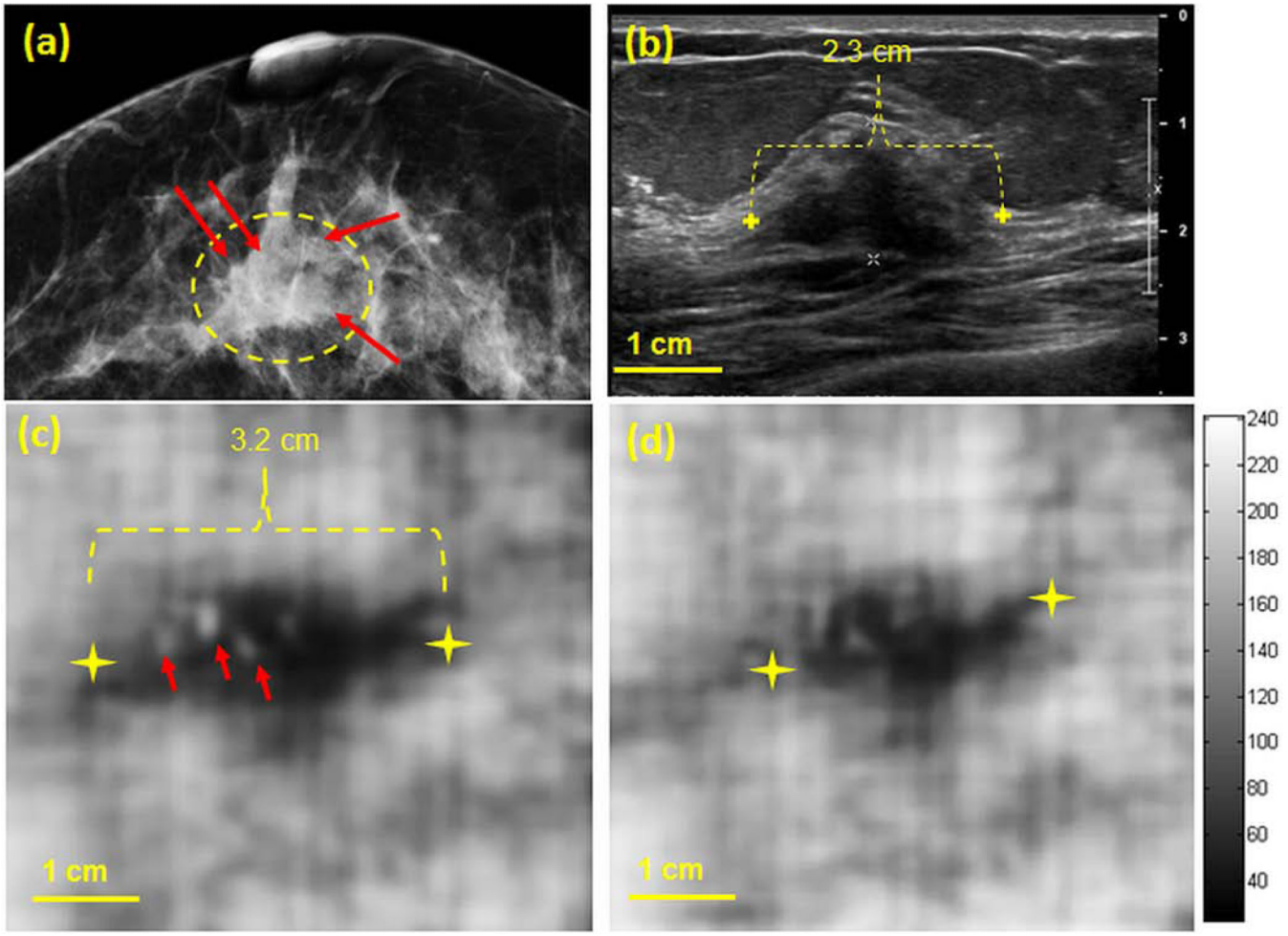


**Figure 3.**

(a) Craniocaudal mammogram of the right breast demonstrates a central focal asymmetry. Microcalcifications are marked with red arrows. (b) Clinical B-mode US shows an irregular 23 mm hypoechoeic mass corresponding to the mammographic abnormality. (c,d) Q2DVA images of breast tissue, obtained by using the Q2D probe, at depths of 25 mm and 27.5 mm, respectively. The lesion is clearly visualized and is marked with yellow markers on panel (c). The presence of calcifications is also noted in the VA image at 25 mm (marked with red arrows).

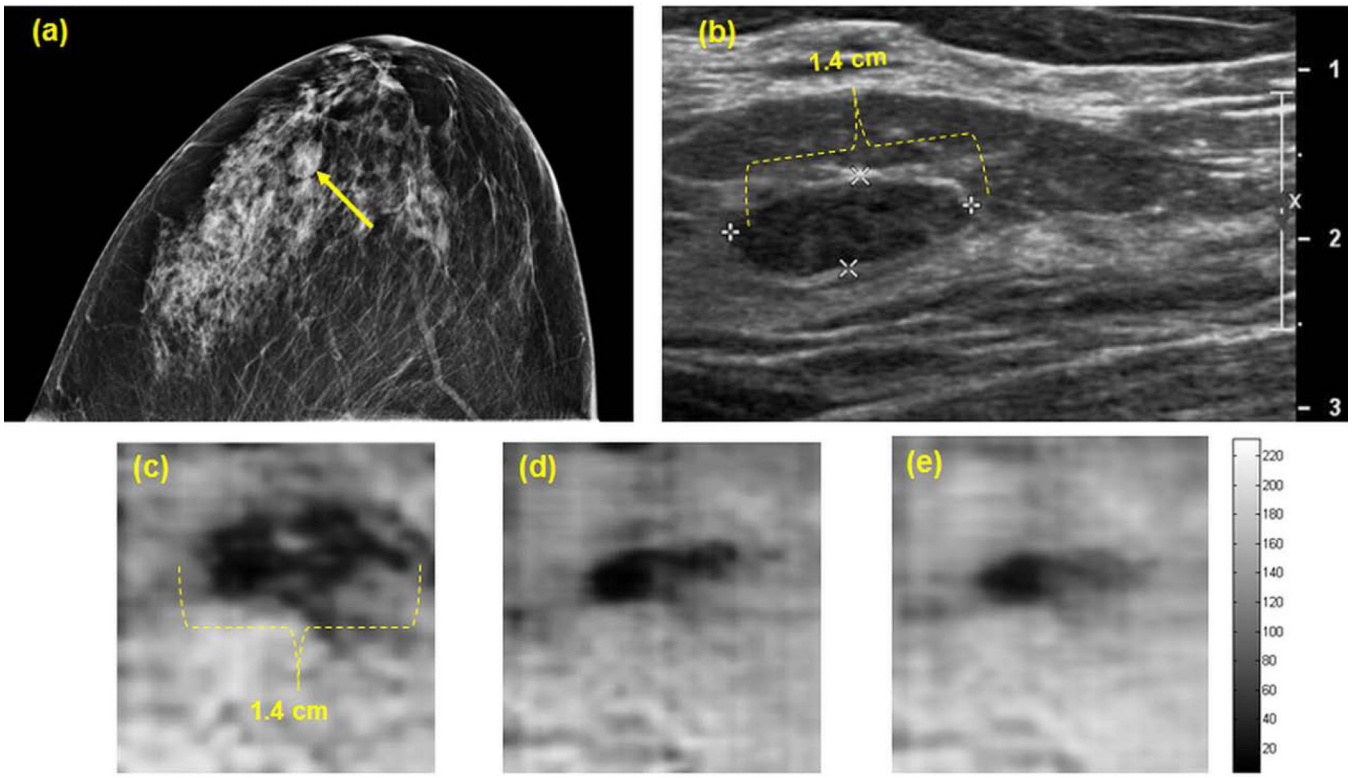


**Figure 4.**

(a) Craniocaudal mammogram demonstrates a small mass in the anterior breast. (b) Clinical B-mode US shows a small corresponding hypoechoic mass. (c-e) Q2DVA images of breast tissue demonstrate a 14 × 6 mm solid mass (fibroadenoma) at depths of 17.5 mm, 20 mm, and 22.5 mm. The mass is well-visualized and size estimates correspond with clinical US measurements.

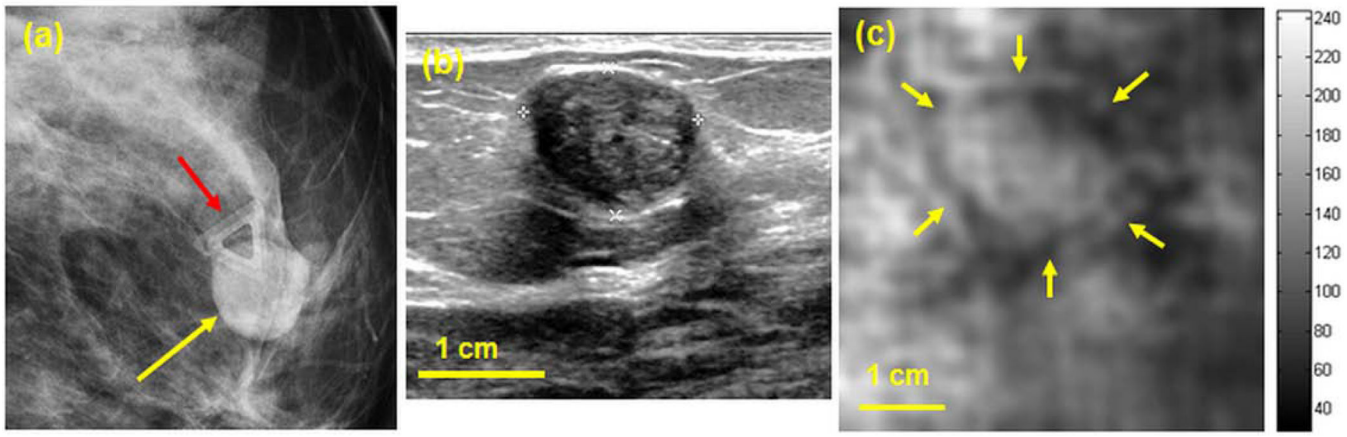


**Figure 5.**

(a) Magnified mediolateral oblique image of the left breast shows a round mass with circumscribed margins at anterior depth. (b) The clinical US image demonstrates the corresponding round mass with mixed internal echogenicity and circumscribed margins. (c) Q2DVA image of the breast outlines the corresponding mass (yellow arrows).

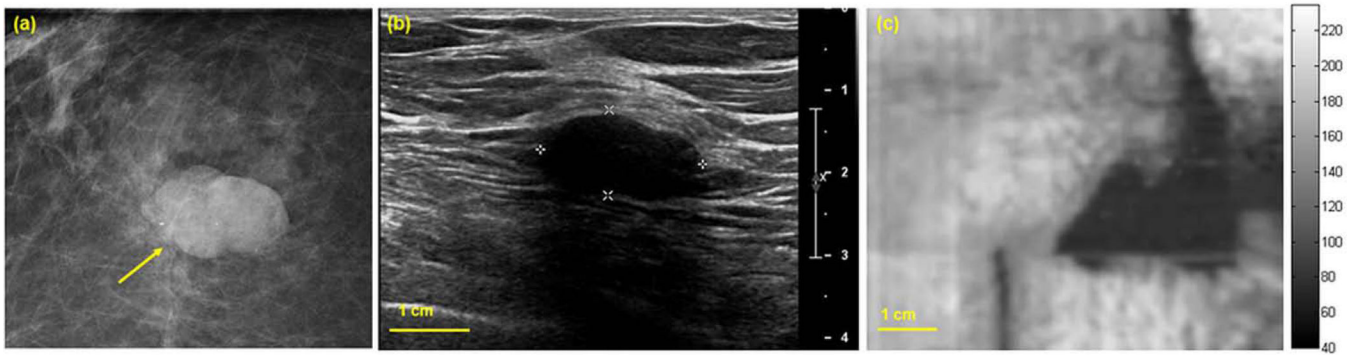


**Figure 6.**

(a) Magnified craniocaudal mammogram shows an oval mass in the posterior depth of the right breast. (b) Clinical B-mode US documents the corresponding mass. (c) Q2DVA image of breast tissue with a sclerosing fibroadenoma at 30 mm depth.

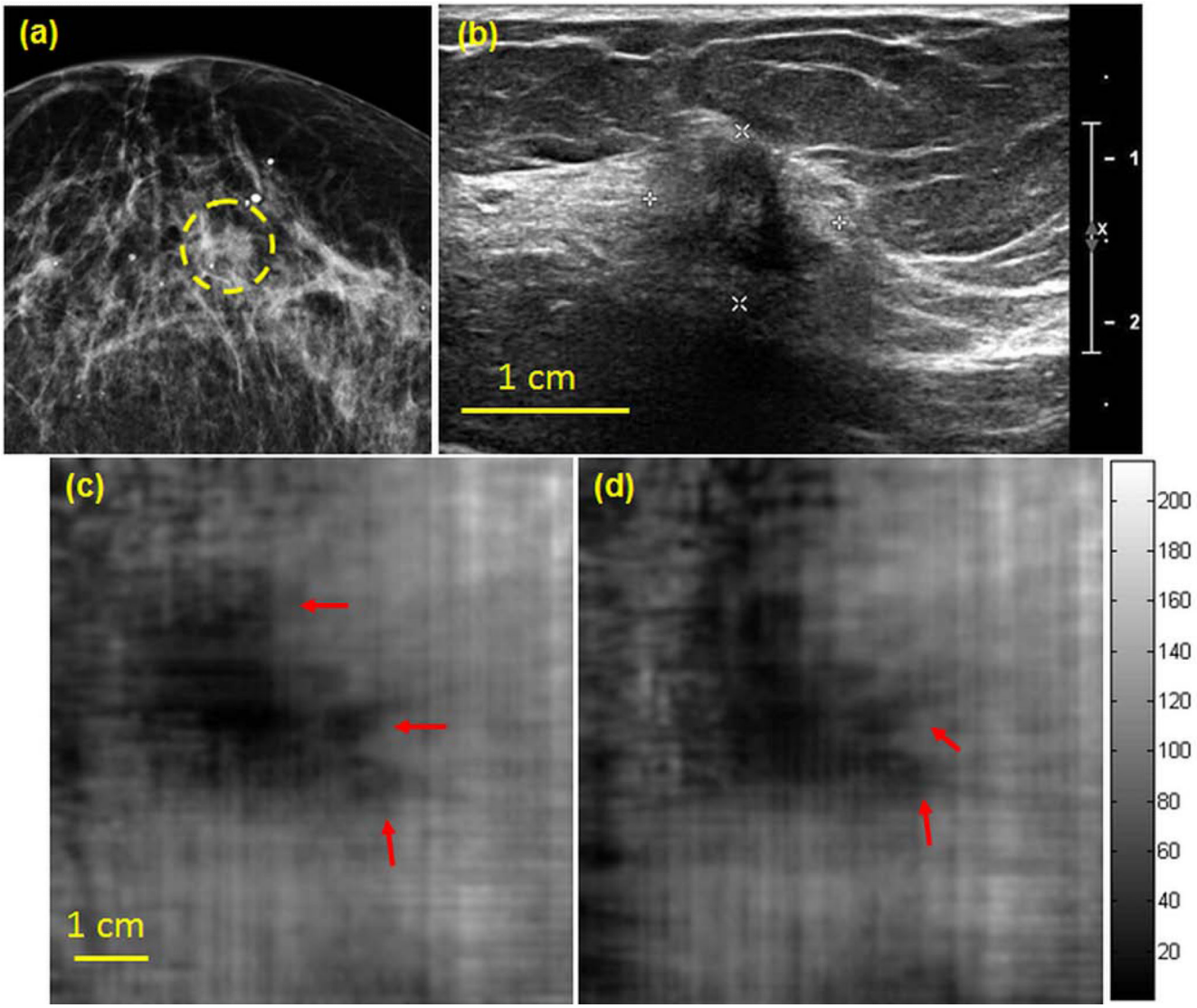


**Figure 7.**

(a) Craniocaudal mammogram demonstrates a possible asymmetry at middle depth. (b) Clinical targeted US image shows an irregular corresponding mass with ill-defined margins with shadowing. (c,d) Corresponding Q2DVA images document the malignancy at 25 mm and 27.5 mm depths. The irregular extension of the mass (marked with red arrows) suggesting suspicious speculations.

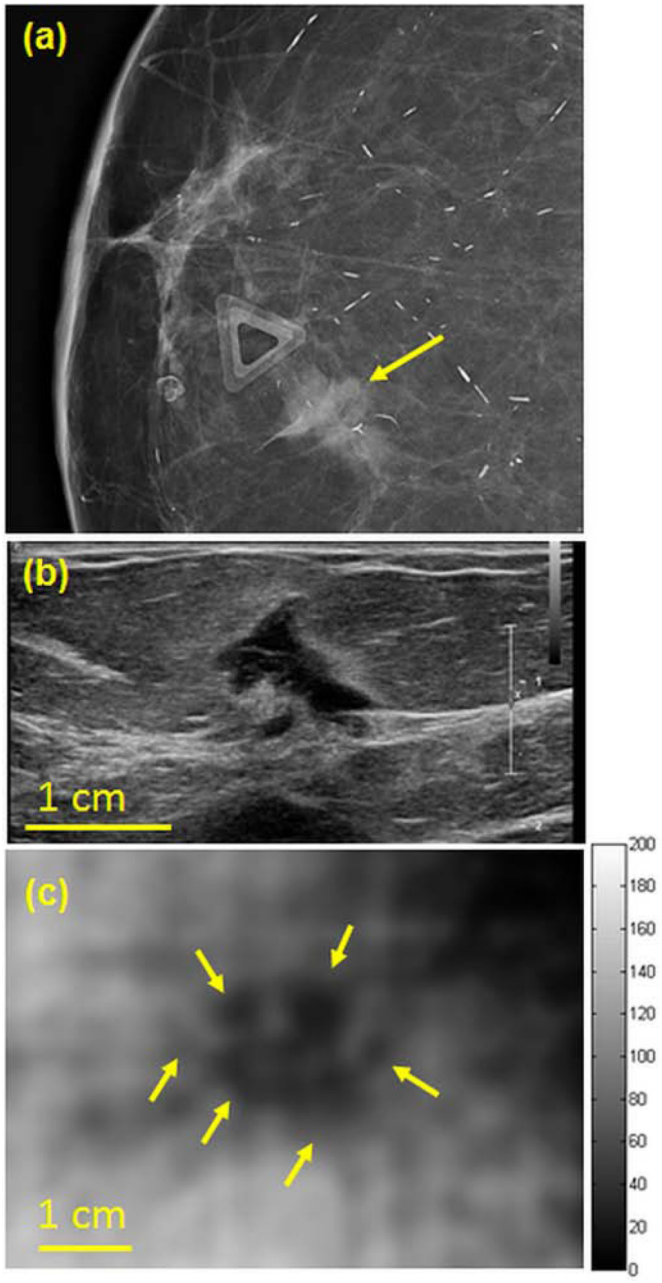


**Figure 8.**

(a) Magnified craniocaudal mammogram demonstrates asymmetry at the anterior depth corresponding to the palpable lump (noted by the triangular skin marker) (b) Clinical targeted US image documents the corresponding mass (c) Corresponding Q2DVA image at a depth of 17.5 mm. The mass with its irregular border is marked with yellow arrows.